Acoustic Doppler Compensation using Feedforward Retiming for Underwater Coherent Transmission

Xiao Liu and Jean-François Bousquet
Electrical and Computer Engineering
Dalhousie University
Halifax, Nova Scotia B3H 4R2
Email: x.liu@dal.ca

***Abstract*—This paper presents a Doppler compensation architecture to maintain a reliable communication link at the receiver in highly mobile applications. It can recover both symbol timing and carrier frequency offset introduced by the Doppler effect. The standard feedback timing recovery loop has been modified into a feedforward architecture to achieve fast timing convergence and power efficiency. The timing error is tracked by a Gardner detector through all samples before decimation. Further, a control unit uses the timing error information to dynamically adjust the sampling time as well as the carrier frequency offset such that the Doppler shift is fully compensated.**

I. Introduction

The Doppler effect has a significant impact on the development of coherent underwater communication systems with high mobility. When sound wave travels through water, the Doppler effect manifests itself in both frequency shift and time scaling. The relative Doppler scaling factor Δ_D is defined as the ratio of velocity of relative movement in v in the direction of propagation (v is positive when the transmitter and receiver are approaching) with respect to the velocity of wave propagation c (1500 m/s in general). Then, for a transmitted single frequency component w_0, the frequency of received signal bearing a frequency shift is equal to

$$w' = (1 + \Delta_D)w_0 \tag{1}$$

In passband communication, modulation with a carrier is used to transmit high speed data in a limited frequency range. At the receiver, an undesirable carrier frequency offset will be present at the output of the down-converter. Consequently, the constellation of the received data will rotate.

Excessive Doppler also results in a scaling of the waveform in the time domain. If the symbol period of the transmitted signal is T_0, the period of received signal T' is given by

$$T' = (1 - \Delta_D)T_0 \tag{2}$$

To track the symbol timing at the receiver, after conversion to baseband, the received signal can be decimated or interpolated at the symbol rate to align at the center of the symbol period. However, in a time varying environment in which the Doppler scaling factor Δ_D is variable, the sampling phase will be shifting slowly off the ideal sampling point due to time-domain compression or dilation. In highly mobile underwater acoustic applications, a frequency shift does not represent the effect of Doppler accurately, and time scaling is a more accurate model. In these conditions, to compensate the Doppler shift, symbol timing recovery must also be realized along with carrier frequency recovery [1].

This paper presents a Doppler compensation method to maintain a reliable communication link at the receiver. It can recover both symbol timing and carrier frequency offset introduced by the Doppler effect.

In conventional Doppler estimation techniques, a known waveform is transmitted in the frame as a preamble. At the receiver, a bank of discrete correlators with different Doppler shifted replicas of the transmitted waveform are implemented. The branch yielding the largest correlation peak is then selected to determine the Doppler estimate [2]. It is a fast parallel algorithm but typically requires significant hardware resources. Another technique is to measure the duration of a received data packet by interleaving known waveforms before and after a data packet [1]. This technique is spectrally inefficient because the known waveform is repeated twice. More importantly, these algorithms do not allow tracking of the timing within a fraction of the symbol period during the frame acquisition as will be proposed in this work.

The first contribution of this work is the analysis and simulation of a timing recovery loop. For this purpose, a feedback timing recovery loop is modified and converted to a feedforward architecture to achieve fast convergence time [3]. The timing errors are tracked using a timing error detector (TED) at the A/D sampling rate before decimation. A control unit uses the timing error information to adjust the sampling clock as well as the carrier frequency offset dynamically such that the Doppler shift can be compensated in real-time.

The symbol timing error detector applied in this paper was first proposed by Gardner [4]. It is a blind (non-data-aided) algorithm and does not require training sequences. This feedforward architecture is designed to be implemented on a programmable hardware such as a field programmable gate array (FPGA), so the hardware complexity and energy efficiency is also taken into consideration.

This paper is organized as follows. In Section II, the problem is described and the received signal on a mobile platform is modeled. The Doppler compensation architecture is discussed in detail in Section III. The simulation results are presented in Section IV, and the final conclusion is discussed

978-0-933957-43-5 ©2015 MTS

in Section V.

II. Problem Statement

In this Section, a key application is described for the Doppler compensation method proposed. A fixed device communicates to an underwater moving platform, such as an autonomous underwater vehicle (AUV). The maximum speed is 30 knots (15.4 m/s), and in this study, the receiver moves towards the transmitter in the direction of propagation. The symbol period is compressed and the carrier frequency will increase according to equations (1) and (2). So Δ_D is about 1%, and for a carrier frequency of 2 kHz, the frequency offset is as much as 20 Hz. The symbol rate is set to 320 Hz and the sampling rate is 10.24 kHz. Therefore, the oversampling rate is 32 samples per symbol.

We consider pulse shaped, coherent phase-shift keying modulated signal transmitting through a white Gaussian noise channel. In this work, a single path arrival is assumed, and in a multipath channel it is expected that the timing recovery proposed will lock onto the main path arrival. The complex representation of the received signal can be written as

$$r\left(t\right)=\sum_{i} c_i g\left(t-iT'-\tau\right) e^{j\left(w't+\theta\right)}+n\left(t\right) \tag{3}$$

where c_i is a sequence of transmitted symbols. A root-raised-cosine pulse $g(t)$ with the rolloff factor β is employed, where its duration is scaled and it has an unknown fractional symbol time offset τ. The frequency of the carrier is also shifted to w' with a phase offset θ. The definition of w' and T' can be found in equations (1) and (2). Additionally, a complex-valued white Gaussian noise is added as $n\left(t\right)$.

After the matched filter, the baseband signal is down-converted by a *fixed* local oscillator, which clock rate is equal to w_0. The baseband signal is given by

$$y\left(t\right)=\sum_{i} c_i h\left(t-iT'-\tau\right) e^{j\left(\Delta_D w_0 t+\theta\right)}+n'\left(t\right) \tag{4}$$

where the pulse denoted by $h(t)$ now becomes a raised-cosine pulse, and $n'(t)$ is a narrowband process. From equation (4), there are two tasks that need to be done before demodulation: compensation of the carrier frequency offset $e^{j\left(\Delta_D w_0 t+\theta\right)}$ and sampling the signal at the scaled symbol rate $1/T'$.

III. Doppler compensation architecture

In this section, the proposed Doppler compensation circuit will be presented. Specifically, in Section III-A the architecture is introduced. In Section III-B, the basic concepts of the Gardner TED is reviewed. Finally, the implementation of the proposed architecture is described in detail in Section III-C.

A. A preview of Doppler compensation architecture

The proposed Doppler compensation architecture is shown in Fig. 1. In the upper branch, the decimator is placed before carrier frequency recovery. With a high oversampling rate, the symbol clock is recovered and aligned dynamically using a feedforward architecture. This technique also avoids interpolations of samples. In this work, decimator working at

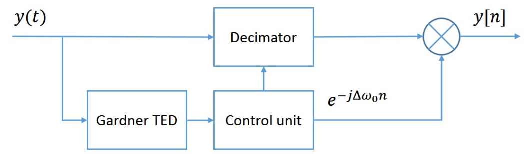

Fig. 1: The proposed Doppler compensation architecture

the sampling rate is placed before carrier recovery, such that the following blocks can work on a much lower symbol clock rate to save energy.

The lower branch in Fig.1 includes the Gardner TED and a control unit. The Gardner TED feeds the error signal to the control unit. The control unit is programmed to adjust a counter which provides the decimator with sampling instances (strobes) at the symbol rate, such that it will sample at maximum eye opening and minimize the intersymbol interference (ISI). Moreover, the control unit also interprets the timing information to generate an estimate of the carrier frequency offset. The output from the decimator is weighed by the carrier frequency offset estimation to compensate it. Thus, the features of the proposed Doppler compensation circuitry are: 1) a feedforward configuration, 2) carrier frequency offset estimation with symbol timing, and 3) a control unit for both symbol timing and carrier recovery.

The next few sections will explain key components of the Doppler compensation circuitry.

B. Gardner timing error detector

The purpose of the timing recovery loop is to obtain symbol synchronization. Two quantities must be determined by the receiver to achieve symbol synchronization. They are sampling frequency $1/T'$ and sampling phase τ. The timing error detector, at the core of timing recovery loop, can generate timing errors which are proportional to the sampling phase offset. There are many types of TEDs in the literature [3], and the Gardner TED has seen widespread use in many practical timing recovery loop implementations. The algorithm uses two samples per symbol and has the advantage of being insensitive to carrier phase offsets. The timing recovery loop can lock first, therefore simplifying the task of carrier recovery. The error for the Gardner algorithm is computed with signal samples $y[n]$ using

$$e[n]=\{y[n]-y[n-M]\}\cdot y[n-M/2] \tag{5}$$

where M is the number of samples per period. Note that in equation (5), one of two samples within one symbol is recycled to the neighbor symbol, so each error calculation uses three samples.

A typical timing recovery loop using a feedback architecture is given in Fig. 2. The signal passes through an interpolator, which is able to generate new samples in between those actually samples when it is triggered by the voltage controlled oscillator (VCO). The output of interpolator is then sent to a Gardner TED. The control signal for the VCO is formed by

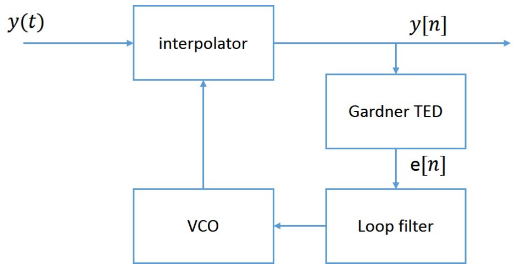

Fig. 2: A standard Gardner timing recovery loop

filtering this error signal using a standard second order loop filter containing a proportional and an integral branch [5].

C. Implementation of Doppler compensation

It has been previously proven in [4] that the performance of the Gardner TED is independent of carrier phase recovery. But its performance with carrier frequency offset is not well documented in the literature. In fact, using similar derivation, it can be proven that in the presence of Δ_D, the error output $e'[n]$ is given by the following equation:

$$e'[n] = \cos\left(\frac{\Delta_D \omega_0 T}{2}\right) e[n] + \sin\left(\frac{\Delta_D \omega_0 T}{2}\right) e''[n] \quad (6)$$

where $e''[n]$ has a similar expression of $e[n]$. Therefore, when Δ_D is less than 1%, $e'[n] \approx e[n]$, the performance degradation is negligible.

The S-curve provides the output of TED $S(\tau)$ at different sampling phase τ. For the Gardner TED, the S-curve is given by [3]

$$S(\tau) = K \sin\left(\frac{2\pi\tau}{T}\right) \quad (7)$$

where the ideal sampling phase is $\tau = 0$. K is a function of T and β, and can be treated as a constant for a certain signal setting. In our architecture, the errors fed by the Gardner TED to the control unit can be analyzed with the S-curve. A decision can be made by waiting for $S(\tau) = 0$. It indicates that $\tau = 0$ is reached at the current sample. However, the Gardner TED also obtains zero values at $\tau = \pm T/2$, in which case a false decision is made. Instead of looking for zeros, considering the sinusoidal curve in equation (7), the decisions should be made at zero-crossing points on the curve where the slope is positive.

Another particularity of the Gardner TED is that it is accurate when the window of interest includes a symbol transition. However, the Gardner error remains relatively small when the current and previous symbol have the same polarity, and this is irrespective of the sampling point.

In this work, to avoid false detection due to no symbol transition, the slope of the error is also evaluated, and compared to a threshold. The clock is re-aligned only when the TED error sequence (averaging may applied when when low SNR) is crossing zero and that the slope is greater than the threshold.

After a sampling decision is made, a configurable counter inside the control unit is re-initialized and set to running. It is reset to zero once its value reaches A/D's oversampling rate (32 in our case), and at this instant, the decimator selects the current sample. The purpose of using a counter is to ensure that no symbol is missing even if there is no decision made from the Gardner TED, particularly when consecutive symbols have the same polarity. Without Δ, the Gardner TED's decisions are always made when the counter is back to zero. By contrast, with Δ, the counter leaps forward or backward by 1 step (to avoid instability) to re-align its zero with the decision instant when they are not aligned. Through this process, although the scaled symbol rate may be a fraction multiple of the A/D sampling rate, the average sampling frequency of decimator is adjusted to $1/T'$.

After symbol timing recovery, the next task is to compensate for the carrier frequency offset. There are several data-aided methods [6] [7] which require ideal symbol timing. Alternatively, in this work, the carrier frequency offset is estimated from the symbol period scaling.

From equation 2, Δ_D can be estimated using

$$\Delta_D = \frac{T_0 - T'}{T_0} \quad (8)$$

The Doppler scaling factor Δ_D can either be smoothed through several symbols or dynamically adjusted symbol by symbol. The output of decimator is then multiplied with $e^{-j\Delta_D w_0 t}$ to compensate for the carrier frequency offset.

IV. Simulation Results

To verify the behaviour of the timing recovery circuit, the performance of the proposed architecture in a white Gaussian noise channel is modeled. The system parameters are described in Section II. To demonstrate Doppler compensation for a constant envelope modulation, QPSK is chosen here. A root-raised-cosine pulse $g(t)$ with a rolloff factor 0.5 is employed. The Doppler scaling factor Δ_D is 1%, and the SNR in the channel is 10 dB. At the receiver, after coarse down-conversion and the matched filter, the baseband signal is processed by the Gardner TED.

Fig. 3 shows the received baseband signal in the in-phase branch, the Gardner TED's output and corresponding sampling decisions for the first ten symbols. As observed in Fig. 3, all sampling decisions are made in the middle of symbols as expected. Also they only appear when the error sequence is crossing zero with a large positive slope in accordance with the algorithm described in Section III. Between symbols 6 and 7, there is no transition, leading the Gardner TED incapable of making a decision. That is where the free running counter inside the control unit becomes useful.

The baseband signal before decimation suffers from undesired phase and amplitude modulation. The job of symbol timing is to define the ideal sampling time to minimize the phase and amplitude variation. Moreover, if a carrier frequency offset is introduced, the scatter plot rotates. Fig. 4 demonstrates the performance of the architecture with scatter plots.

In Fig. 4a, the signal before decimation rotates with various of amplitude. Fig. 4b shows that after retiming decimation,

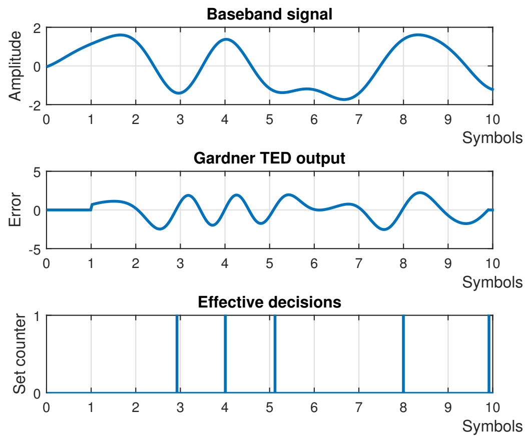

Fig. 3: Baseband signal, Gardner TED's output and corresponding sampling decisions

only samples at the middle of the symbols left, and they are distributed around a rotating constellation with nearly same amplitude. The last step, carrier frequency compensation is shown in Fig. 4c. The samples are aggregated near constellation and the rotation is removed. During these simulations, the carrier phase offset is not considered, and need to be compensated by other blocks. Also, the estimation error of the carrier frequency offset may accumulate after a number of symbols if it is not monitored. Nonetheless, these results can still prove that the proposed architecture can neutralize the symbol period scaling and the carrier frequency shift introduced by the Doppler effect.

V. Conclusion

In this paper, we presented a Doppler compensation architecture for underwater communication. The Doppler effect introduces time scaling and frequency shift which can significantly deteriorate the performance of a communication link. The proposed architecture compensates the symbol period scaling as well as carrier frequency shift. Because underwater water communication systems usually have high oversampling rate, this design avoids using interpolating filters, and thus preserves the signal integrity. Moreover, a feedforward architecture is preferred to a feedback one, to improve convergence time and power efficiency. The Gardner TED processes all data samples and shares its output with a control unit, which can provide both decimation decisions and estimation of the carrier frequency offset.

To recover the transmit information in realistic underwater acoustic propagation conditions, the timing recovery circuit can be combined with an equalizer to optimize the link reliability.

Acknowledgment

The authors would like to thank Ultra Electronics Maritime Systems and NSERC for financial support.

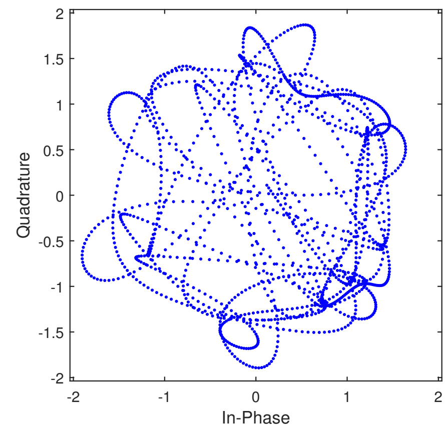

(a) before decimation

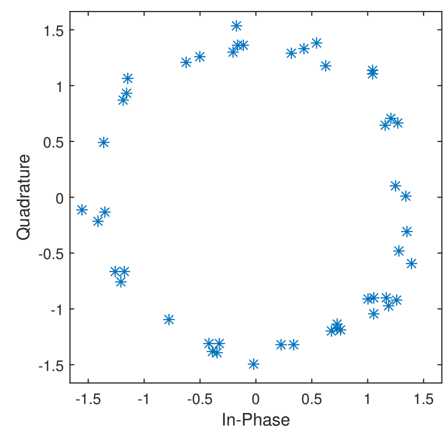

(b) after re-timing

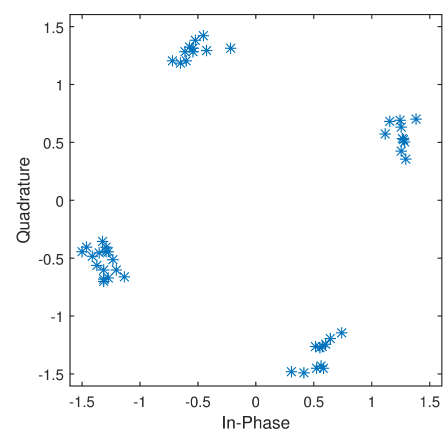

(c) with CFO compensation

Fig. 4: Representation of typical scatter plot at different stages of the receiver

References

[1] B.S. Sharif, J. Neasham, O.R. Hinton, and A.E. Adams, "A computationally efficient doppler compensation system for underwater acoustic communications," *Oceanic Engineering, IEEE Journal of*, vol. 25, no. 1, pp. 52–61, 2000.

[2] M. Johnson, L. Freitag, and M. Stojanovic, "Improved Doppler tracking and correction for underwater acoustic communications," in *1997 IEEE International Conference on Acoustics, Speech, and Signal Processing*. vol. 1, pp. 575–578, IEEE Comput. Soc. Press.

[3] U Mengali and A N D'Andrea, *Synchronization Techniques for Digital Receivers*, Applications of Communications Theory. Springer, 1997.

[4] F. Gardner, "A BPSK/QPSK Timing-Error Detector for Sampled Receivers," *IEEE Transactions on Communications*, vol. 34, no. 5, pp. 423–429, 1986.

[5] F. Gardner, *Phaselock Techniques: Third Edition*, 2005.

[6] M.P. Fitz, "Planar filtered techniques for burst mode carrier synchronization," in *IEEE Global Telecommunications Conference GLOBECOM '91: Countdown to the New Millennium. Conference Record*. 1991, pp. 365–369, IEEE.

[7] U Mengali and M. Morelli, "Data-aided frequency estimation for burst digital transmission," *IEEE Transactions on Communications*, vol. 45, no. 1, pp. 23–25, 1997.